Electronic Supplementary Material (ESI) for Nanoscale

Supporting Information

Wurtzite $CuInS_2$ and $CuIn_xGa_{1-x}S_2$ Nanoribbons: Synthesis, Optical and Photoelectrical Properties

Qiang Li, Lanlan Zhai, Chao Zou,* Xusheng Huang, Lijie Zhang, Yun Yang, Xi'an Chen, Shaoming Huang*

Nanomaterials and Chemistry Key Laboratory, College of Chemistry and Materials Engineering, Wenzhou University, Wenzhou 325027, People's Republic of China

Email: zouchao@wzu.edu.cn, smhuang@wzu.edu

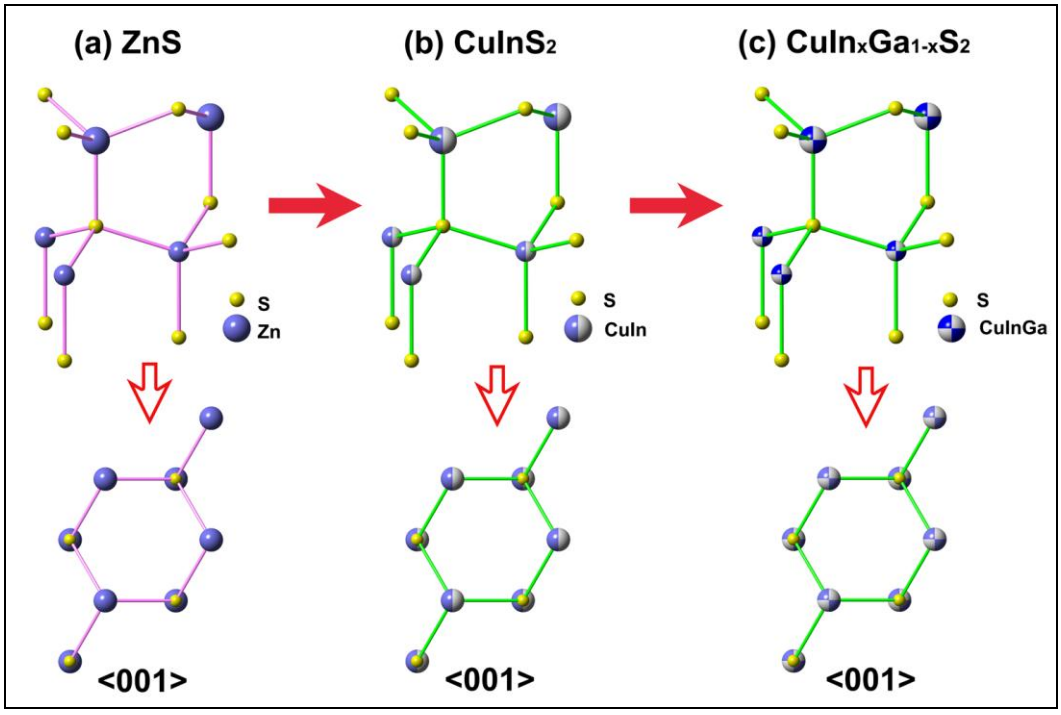

Figure S1. Crystal structure of (a) Wurtzite ZnS, (b) Wurtzite $CuInS_2$, and (c) Wurtzite $CuIn_xGa_{1-x}S_2$. The lower represent crystal structure with zone axis of <001>.

Wurtzite $CuInS_2$ can be obtained by replacing Zn sites in wurtzite ZnS using Cu and In atoms, which occupy the same positions and have the equal occupation 50%. Wurtzite $CuIn_xGa_{1-x}S_2$ can be obtained by replacing Zn sites in wurtzite ZnS using Cu, In, and Ga atoms, which occupy the same positions. Among three atoms, the occupancy of Cu atoms is constant 50%, In and Ga atoms have variable values between 0% to 50%, respectively, depending on the Ga content in $CuIn_xGa_{1-x}S_2$.

Crystal data (Wurtzite)

Formula	$CuInS_2$	$CuIn_xGa_{1-x}S_2$
Space group	$P6_3mc$	$P6_3mc$
Lattice parameter (a)	3.908(0) Å	3.740(0) - 3.908(0) Å
Lattice parameter (c)	6.425(0) Å	6.188(0) - 6.425(0) Å

Atomic positions:

	x	y	z
S	**1/3**	**2/3**	**0**
	2/3	**1/3**	**1/2**
Cu/In/Ga	**1/3**	**2/3**	**0.375**
	2/3	**1/3**	**0.875**

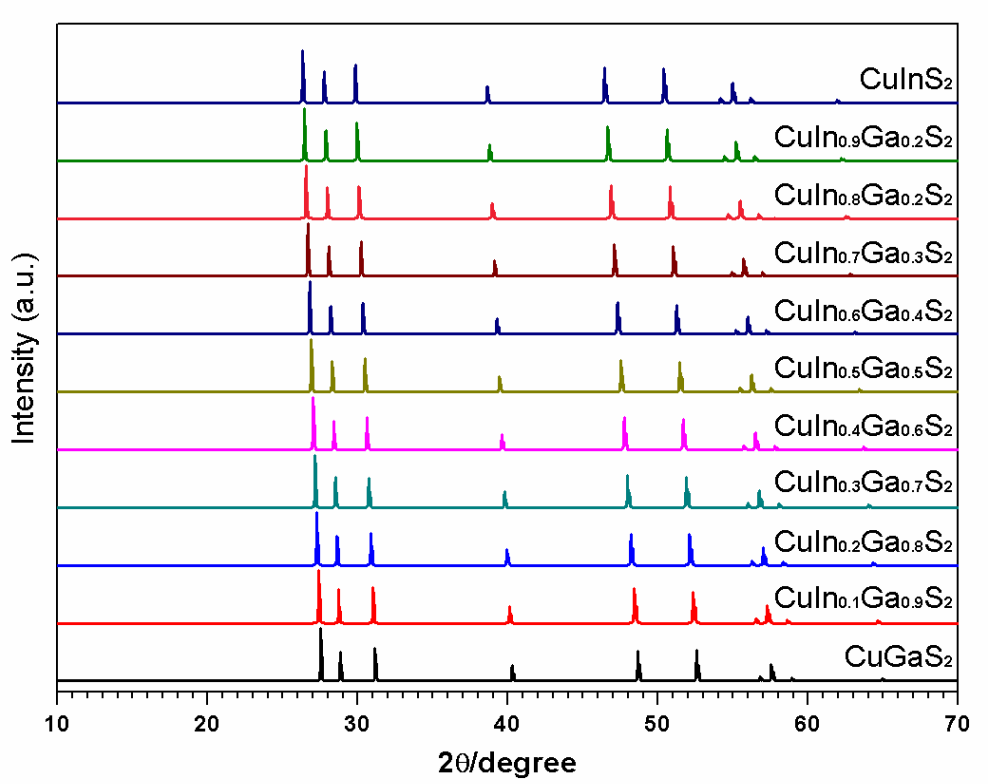

Figure S2. The simulated XRD pattern of wurtzite $CuInS_2$, $CuGaS_2$, and $CuIn_xGa_{1-x}S_2$.

Table S1 Calculated interplanar distance and the corresponding mismatch between wurtzite $CuIn_xGa_{1-x}S_2$ and roxbyite $Cu_{1.75}S$

	Wurtzite $CuIn_xGa_{1-x}S_2$						Roxbyite $Cu_{1.75}S$			Mismatch1	Mismatch2	Mismatch3
X value	**a**	**c**	**[100]**	**[110]**	**[$1\bar{1}0$]**	**[002]**	**[0160]**	**[$\bar{1}6\bar{0}0$]**	**[004]**	**[110]||[0160]**	**[$1\bar{1}0$]||[$\bar{1}6\bar{0}0$]**	**[002]||[004]**
$CuInS_2$	3.908	6.425	3.38443	1.954	3.38443	3.2125	1.93125	3.3618	3.34	1.18%	0.67%	-3.82%
0.9	3.8912	6.4013	3.36988	1.9456	3.36988	3.20065	1.93125	3.3618	3.34	0.74%	0.24%	-4.17%
0.8	3.8744	6.3776	3.35533	1.9372	3.35533	3.1888	1.93125	3.3618	3.34	0.31%	-0.19%	-4.53%
0.7	3.8576	6.3539	3.34078	1.9288	3.34078	3.17695	1.93125	3.3618	3.34	-0.13%	-0.63%	-4.88%
0.6	3.8408	6.3302	3.32623	1.9204	3.32623	3.1651	1.93125	3.3618	3.34	-0.56%	-1.06%	-5.24%
0.5	3.824	6.3065	3.31168	1.912	3.31168	3.15325	1.93125	3.3618	3.34	-1.00%	-1.49%	-5.59%
0.4	3.8072	6.2828	3.29713	1.9036	3.29713	3.1414	1.93125	3.3618	3.34	-1.43%	-1.92%	-5.95%
0.3	3.7904	6.2591	3.28258	1.8952	3.28258	3.12955	1.93125	3.3618	3.34	-1.87%	-2.36%	-6.30%
0.2	3.7736	6.2354	3.26803	1.8868	3.26803	3.1177	1.93125	3.3618	3.34	-2.30%	-2.79%	-6.66%
0.1	3.7568	6.2117	3.25348	1.8784	3.25348	3.10585	1.93125	3.3618	3.34	-2.74%	-3.22%	-7.01%
$CuGaS_2$	3.74	6.188	3.23894	1.87	3.23894	3.094	1.93125	3.3618	3.34	-3.17%	-3.65%	-7.37%

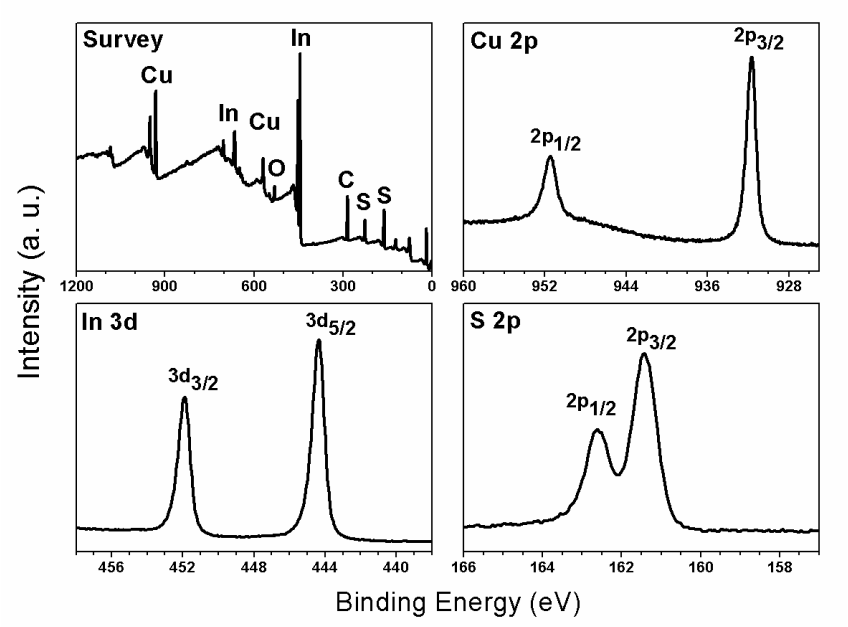

Figure S3. XPS survey spectra of $CuInS_2$ nanoribbons. Peaks assignable to core levels of Cu 2p, In 3d, S 2p, O 1s and C 1s are identified.

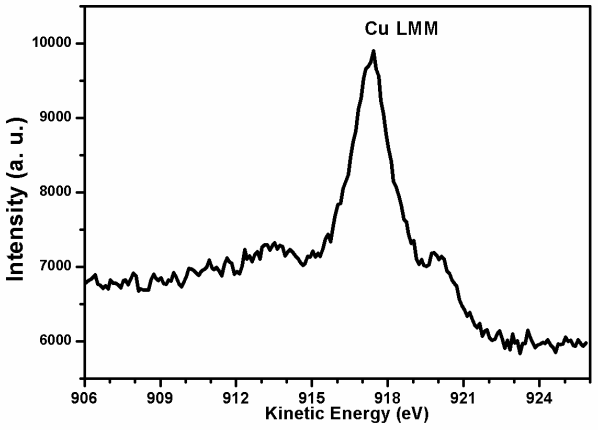

Figure S4. AES spectrum in the Cu LMM region for $CuInS_2$ nanoribbons.

The chemical composition and the oxidation state of $CuInS_2$ nanoribbons were evaluated from XPS and AES. The survey spectrum, high-resolution spectra of Cu 2p, In 3d and S 2p core levels of $CuInS_2$ nanoribbons are shown in Figure S2. Peaks assignable to core levels of Cu 2p, In 3d, S 2p and C 1s are identified in survey spectrum. The high-resolution spectrum of Cu 2p reveals that two peaks are centered at 931.8 and 951.6 eV, respectively, indicative of Cu(I) with a splitting of 19.8 eV, in agreement with the previous reports. Considering the proximity of binding energies for Cu(0) and Cu(I), the unambiguous copper oxidation could not be ascertained. To address the issue, Cu LMM Auger spectroscopic measurement was used to prove the oxidation state of copper in $CuInS_2$ nanoribbons. Shown in Figure S3, the kinetic energy of Cu LMM is centered at 917.2 eV, well consistent with the literature values for Cu(I). The indium $3d^{5/2}$ and $3d^{3/2}$ peaks appear at 444.4 eV and 451.9 eV, indicating In(III). The two peaks of sulfur 2p are located at 161.6 eV and 162.7 eV, respectively, showing a peak separation of 1.1 eV, which are also consistent with the literature value in metal sulfide.

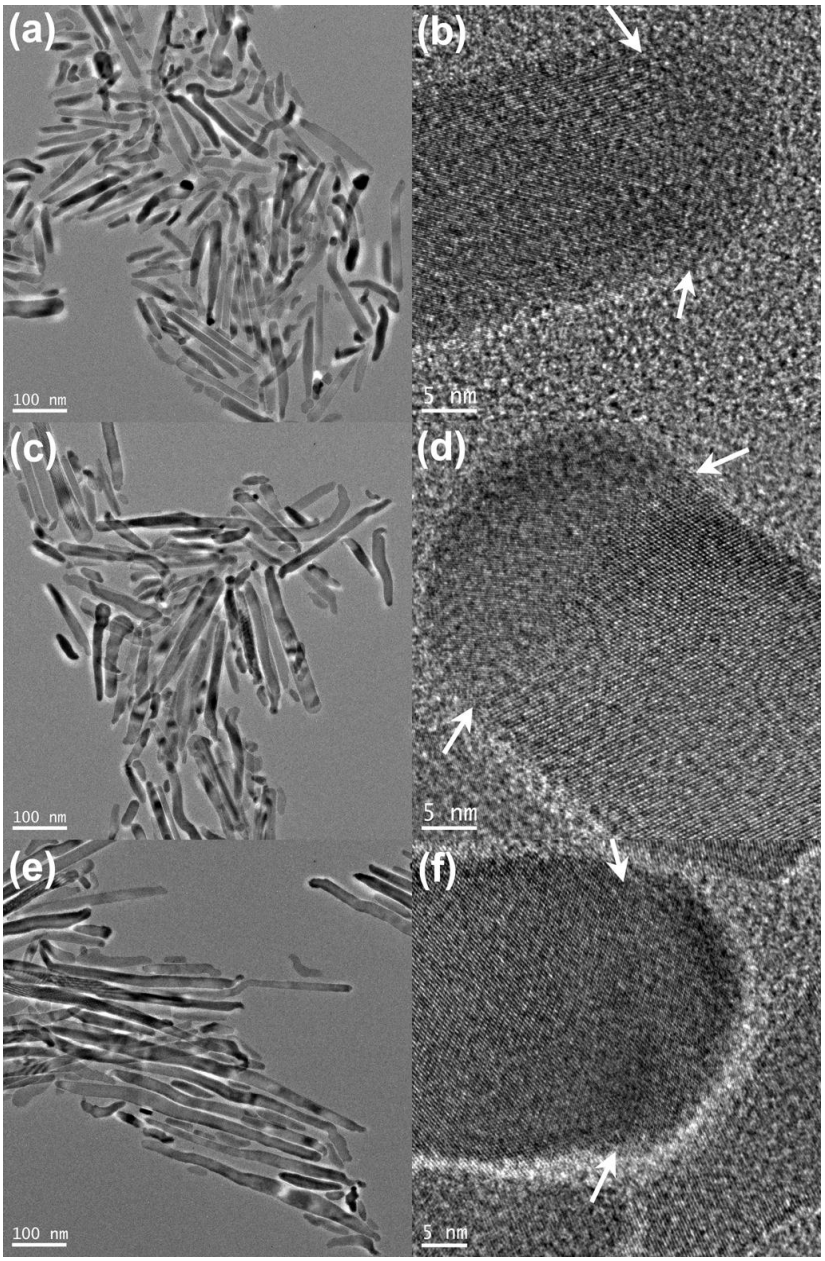

Figure S5. TEM images of $CuInS_2$ nanoribbons during the growth process. (a, b) t = 8 min. (c, d) t = 12 min. (e, f) t = 20 min. White arrow refers to the interface between the $Cu_{1.75}S$ head tip and $CuInS_2$ body of nanoribbons.

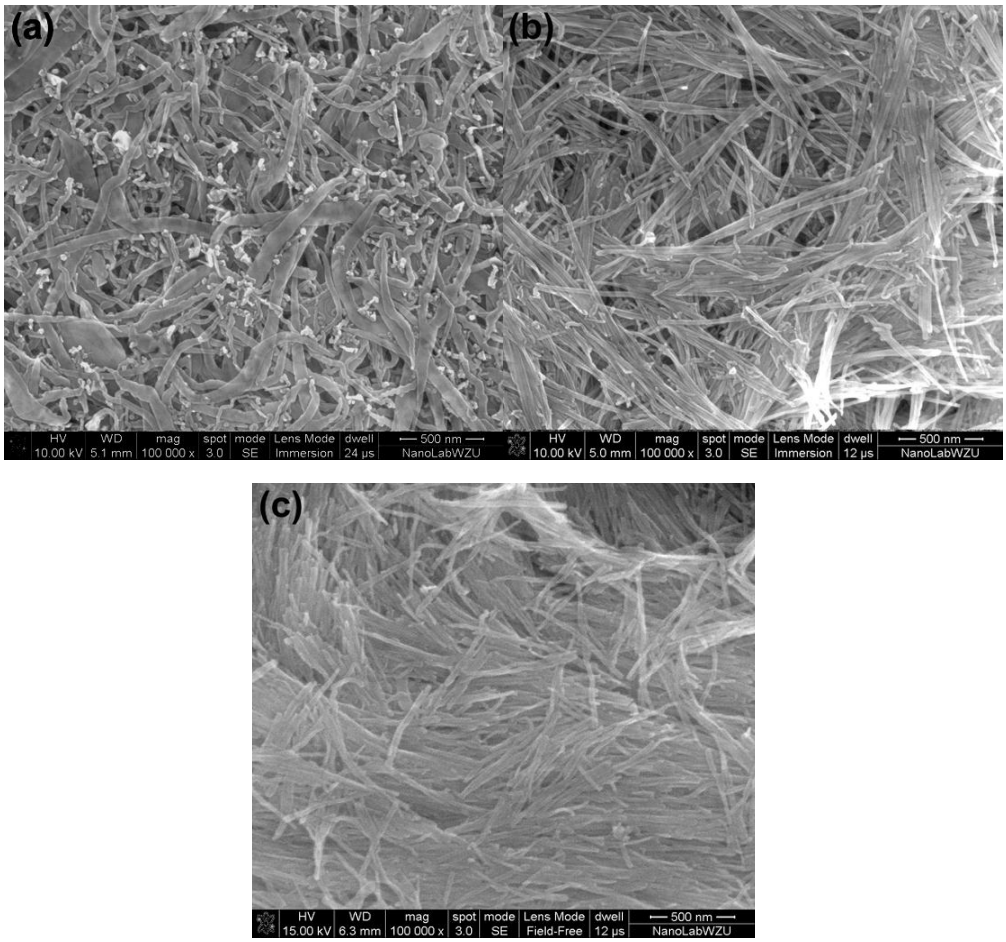

Figure S6. SEM images of quaternary $CuIn_xGa_{1-x}S_2$ nanoribbons. (a) x = 0.2. (b) x = 0.6. (c) x = 0.8.

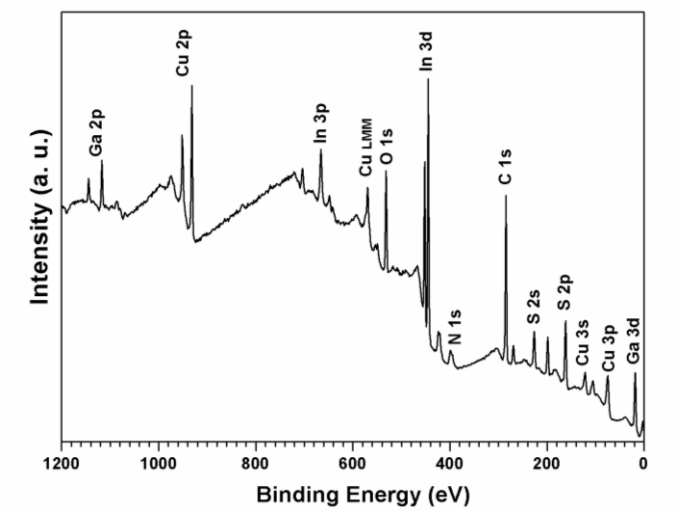

Figure S7. XPS survey spectra of $CuIn_xGa_{1-x}S_2$ nanorods. Peaks assignable to core levels of Cu 2p, In 3d, Ga 2p, S 2p, O 1s, N 1s and C 1s are identified.

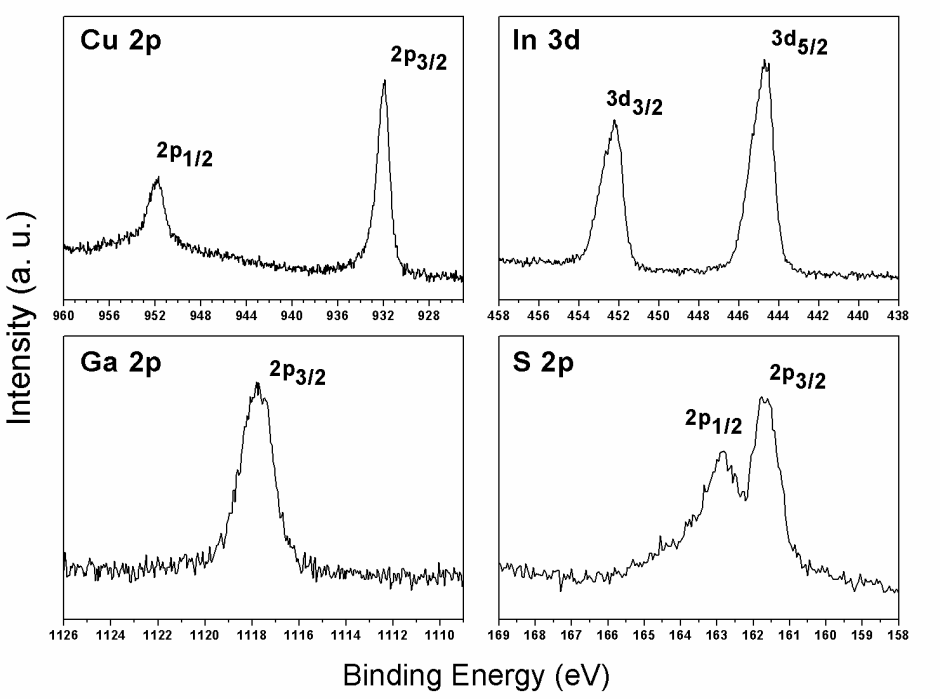

Figure S8. High-resolution of XPS analysis of quaternary $CuIn_xGa_{1-x}S_2$ nanoribbons. In high-resolution spectrum of Cu 2p, two peaks at 932.0 and 951.8 eV appear, indicative of Cu(I) with a splitting of 19.8 eV, which is well consistent with standard separation of 19.8 eV. The In(III) is confirmed by a peak splitting of 7.6 eV, two peaks located at 444.6 and 452.2 eV, respectively. The gallium $2p^{3/2}$ peaks located at 1117.7 eV, indicating Ga(III). The two peaks of sulfur 2p are located at 161.7 and 162.8 eV, respectively, showing a peak separation of 1.1 eV, which are also consistent with the literature value in metal sulfide.

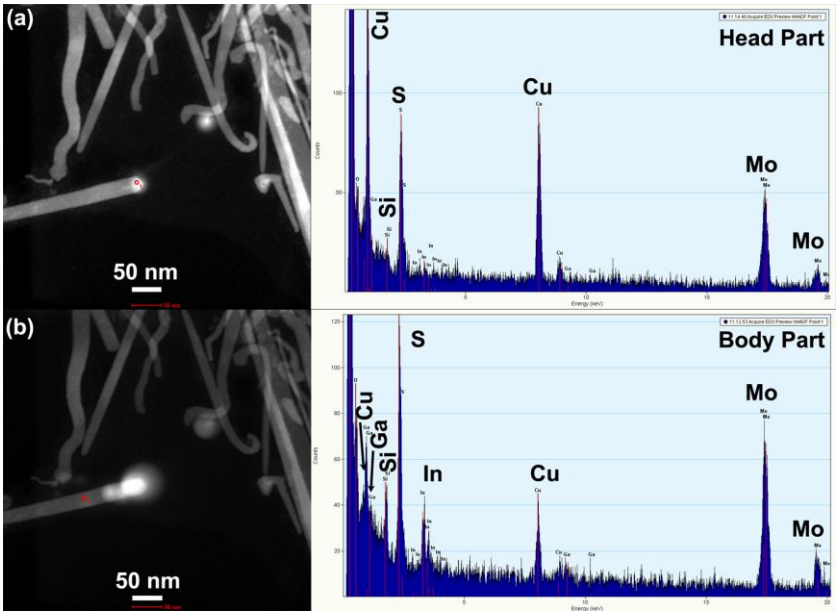

Figure S9. EDS spectra of $CuIn_xGa_{1-x}S_2$ nanoribbons (taken in the TEM) (a) head part, (b) body part. The Mo, Si, and C elements are attributed to molybdenum grid, silicon detector, and carbon film, respectively.

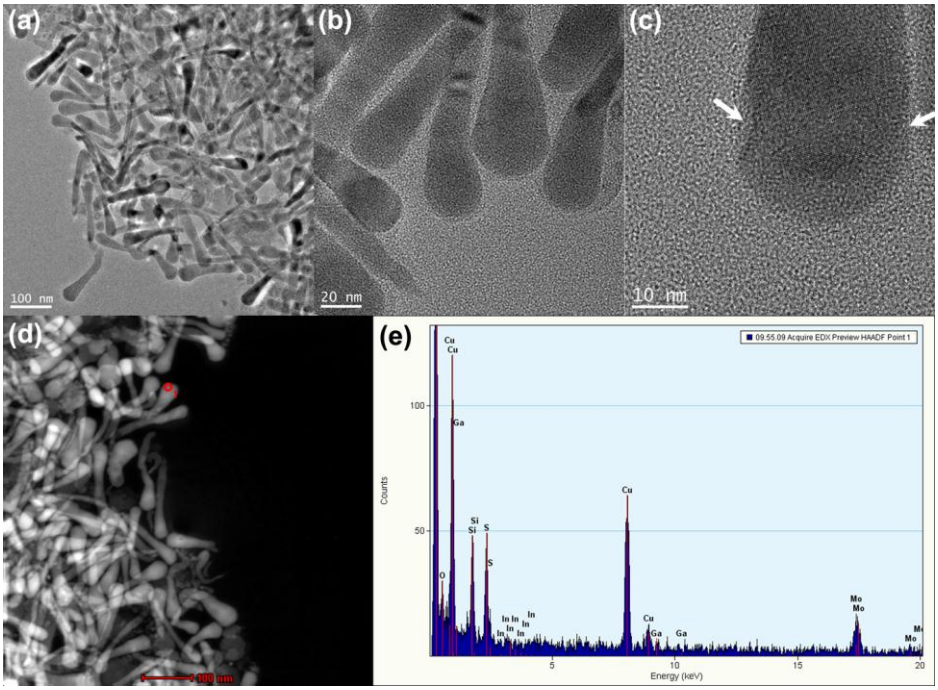

Figure S10. TEM images of $CuIn_xGa_{1-x}S_2$ nanorods with tadpole shape. (a, b, c) TEM images. White arrows represent the interface between the head and the body of nanorod. (d) STEM image. (e) EDS spectrum of the head in $CuIn_xGa_{1-x}S_2$ nanorods (taken from the red circled area in d). The Mo, Si, and C elements are attributed to molybdenum grid, silicon detector, and carbon film, respectively.

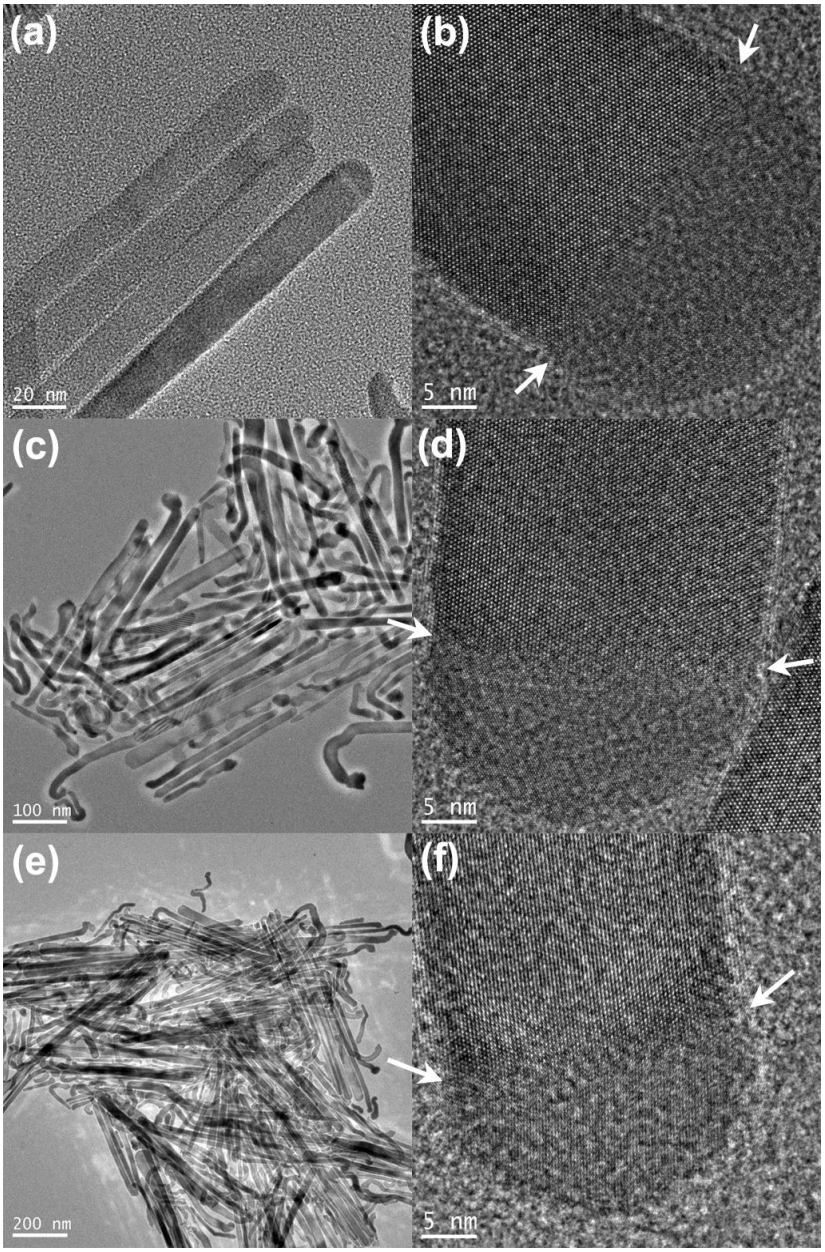

Figure S11. Growth evolution process of the quaternary $CuIn_xGa_{1-x}S_2$ nanoribbons. (a, b) t = 8 min. (c, d) t = 12 min. (e, f) t = 20 min. White arrow refers to the interface between the $Cu_{1.75}S$ head tip and $CuIn_xGa_{1-x}S_2$ body of nanoribbons.